The Amplitude Asymmetry between Synoptic Cyclones and Anticyclones: Implications for Filtering Methods in Feature Tracking

AARON DONOHOE AND DAVID S. BATTISTI

Department of Atmospheric Sciences, University of Washington, Seattle, Washington

(Manuscript received 23 October 2008, in final form 14 May 2009)

ABSTRACT

The ''background'' state is commonly removed from synoptic fields by use of either a spatial or temporal filter prior to the application of feature tracking. Commonly used spatial and temporal filters applied to sea level pressure data admit substantially different information to be included in the synoptic fields. The spatial filter retains a time-mean field that has comparable magnitude to a typical synoptic perturbation. In contrast, the temporal filter removes the entire time-mean field. The inclusion of the time-mean spatially filtered field biases the feature tracking statistics toward large cyclone (anticyclone) magnitudes in the regions of climatological lows (highs). The resulting cyclone/anticyclone magnitude asymmetries in each region are found to be inconsistent with the unfiltered data fields and merely result from the spurious inclusion of the time-mean fields in the spatially filtered data. The temporally filtered fields do not suffer from the same problem and produce modest cyclone/anticyclone magnitude asymmetries that are consistent with the unfiltered data. This analysis suggests that the weather forecaster's assertion that cyclones have larger amplitudes than anticyclones is due to a composite of a small magnitude asymmetry in the synoptic waves and a large contribution from inhomogeneity in the background (stationary) field.

1. Introduction

Hand-drawn analyses of mean sea level pressure (SLP) data and the tracking of synoptic features was the original form of weather forecasting and has been carried out for over a century (Köppen 1881), because synoptic storms exert a profound influence on the day-to-day weather experienced by mankind. They also play a key role in transporting heat in the climate system. It has long been understood that cyclones and anticyclones form, grow, and propagate in certain regions of the Northern Hemisphere (Klein 1957) and that these regions of enhanced storm activity have come to be known as storm tracks.

With the advent of global, gridded, digital atmospheric data systems, the classification of storm tracks shifted away from the tracking of systems based on hand-drawn analyses toward definitions based on the bandpassed Eulerian variance, which is meant to emphasize the magnitude of variability at synoptic time scales (Blackmon et al. 1984). More recently, there has been a resurgence of the feature tracking perspective of storm tracks and automated feature tracking algorithms have been developed to carry out analyses similar to the original hand-drawn analyses but with less human labor and objectively (e.g., Hoskins and Hodges 2002; Blender et al. 1997). The feature tracking and Eulerian perspectives offer different conceptual definitions of storm tracks that are suited for answering different physical questions. Both perspectives are useful and complementary.

Most studies that use feature tracking are concerned mainly with the path and frequency of occurrence of cyclones (Carse and Serreze 1997; Wernli and Schwierz 2006). More recently, studies have attempted to diagnose storm intensity and growth from the feature tracking perspective (Hodges et al. 2003; Hoskins and Hodges 2005; Donohoe and Battisti 2009). Used in this manner, feature tracking directly addresses questions of ensemble storm growth over baroclinic regions and the magnitude of storms seeding the storm tracks. These diagnostics provide insight on how modeled and observed midlatitude cyclone growth and decay are affected by changes in the mean state over the seasonal cycle, anthropogenic climate change, and paleoclimate

Corresponding author address: Aaron Donohoe, University of Washington, 408 ATG Building, Box 351640, Seattle, WA 98195.
E-mail: aaron@atmos.washington.edu

DOI: 10.1175/2009MWR2837.1

states. Eulerian analysis does not directly address the growth of individual systems and thus cannot be used to determine whether storms grow more rapidly in certain spatial regions or climate states than others.

The use of feature tracking to assess storm magnitude and growth is complicated by the fact that feature magnitude is contingent upon the method used to separate the disturbance from the mean state. For instance, the central pressure of a midlatitude cyclone may drop because of cyclone deepening or migration into a large-scale stationary low. The separation of these two effects has no statistical basis in the literature and is complicated by the fact that the climatological surface low pressure regions are thought to be, at least in part, a reflection of the ''ensemble of synoptic lows moving into the region'' (Hoskins and Hodges 2002). The presumed assumption to this logic is that there is an asymmetry between the probability distribution function of cyclone intensity and anticyclone intensity with cyclones more frequently obtaining larger magnitudes than their anticyclone counterparts in the regions of climatological low pressure.

It has long been acknowledged that differences in the intensities and tracks of cyclones and anticyclones are primarily a reflection of and almost inseparable from the climatological mean field (Wallace et al. 1988). In the raw SLP data, cyclones (anticyclones) tend to track northeast (southeast) toward and obtain minimum (maximum) central pressures in the climatological low (high) pressure regions: the Aleutian and Icelandic lows (the Pacific and Bermuda or Azores highs). Thus, in the raw fields, climatological lows (highs) are regions of enhanced synoptic-scale cyclonic (anticyclonic) activity by virtue of the time mean of the field alone. Independent of inhomogeneity in the background field, there are dynamical reasons for expecting asymmetry in the amplitude distribution of cyclones and anticyclones; gradient wind balance, vortex stretching (Holton 2006), surface quasigeostrophic theory (Hakim et al. 2002), and semigeostrophic theory that accounts for ageostrophic vorticity (Snyder et al. 1991) all give a dynamical basis for expecting asymmetry in the amplitude of cyclones and anticyclones in favor of enhanced cyclone activity in the baroclinic zone, which thus suggests that at least part of the time-mean field in the climatological lows is a reflection of this asymmetry. However, other studies suggest that in the regions of cyclonic (anticyclonic) barotropic wind shear north (south) of the jet maximum, cold (warm) frontogenesis is favored (Wernli et al. 1998) and thus provides a theoretical basis for a spatial dependence of the cyclone/anticyclone asymmetry and the associated contribution of synoptic waves to the time-mean SLP field. Whether the climatological mean SLP map is due to the dynamical processes leading to intrinsic asymmetry in the magnitude of cyclones and anticyclones or it represents semipermanent large-scale features that are largely independent of synoptic motions has largely been predetermined by ad hoc definitions applied in the analysis and is still a subject of debate; it is the central issue in this paper.

To perform feature tracking analysis, several recent studies have removed the background state from the raw data prior to application of the tracking algorithm. Anderson et al. (2003) explored how different definitions of the background state affected feature tracking statistics. They found that either the removal of climatology or the application of a temporal high-pass filter resulted in feature tracking statistics that had nearly symmetric amplitudes for cyclones and anticyclones and that the cyclone tracks were zonally oriented and reminiscent of a baroclinic waveguide (Wallace et al. 1988). In contrast, when they filtered out large-scale spatial structures, there was a large asymmetry in the amplitude of synoptic cyclones and anticyclones and the cyclones (anticyclones) tended to track to the northeast (southeast). Their a priori expectation was that cyclones and anticyclones have different magnitudes and different trajectories; hence, they concluded that the spatial filter behaved properly. Here, we compare feature tracking statistics from spatially and temporally filtered data to reexamine the conclusions of Anderson et al. (2003). In particular, we ask whether the amplitude asymmetry in the cyclones and anticyclones found in the feature tracking analysis by using the spatial filter is inherent in the data or if it is an artifact of filter. Although the analysis presented in the current work is limited to SLP, similar analysis has been performed on different fields at different levels and many of the conclusions reached in the present work can be generalized to other fields of interest in feature tracking. Because the choice of how the background state is removed also influences the asymmetry in magnitude between cyclones and anticyclones, we will also directly address in our study the more fundamental question of how different the ensemble of cyclone amplitudes is from the ensemble of anticyclone amplitudes within the storm-track region.

The paper is outlined as follows: in section 2, we introduce the data and filtering techniques used in this study. Two different (one spatial and one temporal) filtering routines that are commonly used prior to feature tracking are summarized, and the impact of the filters on the spatiotemporal variance admitted into the tracking algorithm is discussed. The results from feature tracking using the two different filters is presented in section 3, with an emphasis on the probability distribution function of cyclone and anticyclone magnitude

resulting from the application of the different filters. Here, we find that much of the cyclone/anticyclone magnitude asymmetry found in the spatially filtered fields can be directly attributed to the time-mean field that is retained when the spatial filter is used; it is not due to intrinsic dynamical processes associated with synoptic disturbances. We attempt to partition the Eulerian time-mean field into a part resulting from stationary features and a part resulting from the net effect of passing disturbances by applying a skew-normal distribution to the Eulerian data in section 4, and we show that the cyclone/anticyclone asymmetry makes only a minor contribution to the time-mean field in the storm-track regions. A summary and discussion follow.

2. Data, techniques, and filter properties

The data used in this study are 6-hourly sea level pressure data from the 40-yr European Centre for Medium-Range Weather Forecasts (ECMWF) Re-Analysis (ERA-40; Uppala et al. 2005) at a horizontal resolution of T62.[1] We limit our analysis to data from the satellite era (from 1979 to 2002) and over the cold season extending from 1 November to 31 March (NDJFM). Only the Northern Hemisphere is considered in this paper.

The feature tracking algorithm is well documented by Hodges (1995, 1999) and will only be briefly discussed here. At each time step, features are identified based on smoothing the original data on the sphere and locating spatial extrema in the interpolated field (Hodges 1995). For many input fields, some form of data preprocessing to remove a ''background'' field is necessary; this point is discussed extensively toward the end of the current section. A feature is identified if it exceeds a threshold amplitude of ± 3 hPa, and it is determined to be connected to features at different time steps by minimizing an adaptively constrained cost function that requires the tracks of storms to be smooth (there are not rapid changes in the velocity or magnitude of the features; Hodges 1999). Only features that last for at least 3 days, travel more than 1000 km, and occur within the NDJFM season are retained for analysis.

To identify synoptic-scale extrema in fields that have large-scale spatial structures (such as SLP) it is necessary to remove the ''background distribution'' (Hoskins and Hodges 2002). The impact of the form of background state removal on feature tracking statistics is studied here by comparing two different prefiltering routines: a spatial filter that removes features of planetary wavenumber 5 and less and a temporal filter that removes variability with periods less than 20 days. The steps in spatially filtering the data are as follows: (i) project the raw data onto a spherical harmonic transform with a triangular truncation of 42 planetary wavenumbers; (ii) set to zero the spectral coefficients for total wavenumbers ≤ 5; and (iii) perform the inverse spherical harmonic transform on the modified spectral coefficient. This spatial filter is similar to that used by Hoskins and Hodges (2002, 2005) and Anderson et al. (2003), and it is designed to be conservative: disturbances that have spatial scales typical of synoptic waves should not be affected by the filter. The temporal filter is a sixth-order double-pass Butterworth filter with a cutoff period of 20 days; it is applied to annual data to prevent spurious end effects. The cutoff period was chosen to be conservative in the same sense as the spatial filter; disturbances that have time scales typical of synoptic waves should not be affected by the filter. For temporal signals with time scales less than the cutoff period, the temporal filter passes any skewness perfectly. By definition, the time mean of the temporally filtered data is zero, whereas the time mean of the spatially filtered data is the component of the time-mean field that is smaller scale than 1 over wavenumber 5 (the latter is shown in Fig. 2, bottom).

The commonality and differences between the spatial and temporal filters can be assessed visually by plotting the wavenumber–frequency power spectrum of the NDJFM SLP. A single winter season spectra is generated as follows: (i) reflect the Northern Hemisphere data about the equator; (ii) calculate the spherical harmonic transform of the SLP field at each time frame of the 60-day winter window; (iii) normalize the spectral coefficients so that each spherical harmonic has unit spatial variance (area weighted); (iv) calculate the Fourier transform of the time series of a single spherical harmonic coefficient to get a frequency power spectra associated with that spherical harmonic component; and (v) sum the frequency power spectra from each of the spectral coefficients with the same planetary wavenumber in quadrature to get the power associated with a single frequency and planetary wavenumber. The frequency–planetary wavenumber power spectrum for individual winters are then averaged, and the result is shown in Fig. 1. Because the spectra are red (low-frequency spectral components contain a large portion of the variance), we have plotted the spectrum in natural log frequency space and have multiplied the spectral power by frequency such that the frequency spacing times plotted power is conserved via the relationship

[1] We have also preformed the same analysis presented here with daily averaged sea level pressure from the National Centers for Environmental Prediction reanalysis dataset (Kalnay et al. 1996), and all the conclusions presented here are unchanged.

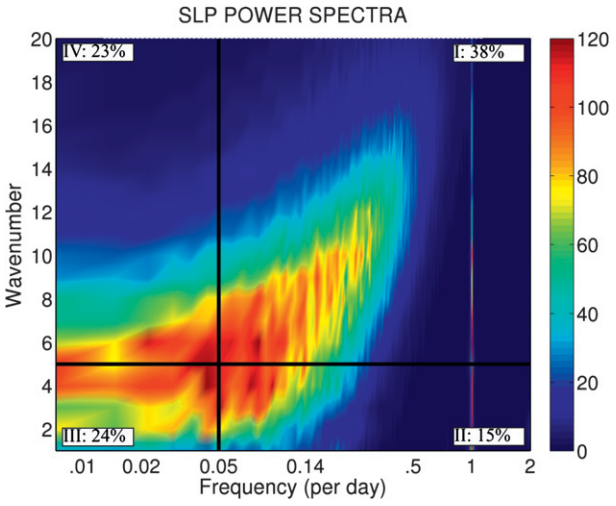

FIG. 1. Power spectrum of NDJFM SLP in natural log frequency–wavenumber space (Pa^2 day^{-1} per discrete spectral realization). The plotting convention is discussed in the text. The thick, black, horizontal (vertical) line represents the boundary of the spatial (temporal) filter. The four quadrants are labeled and discussed in the text; the percent of total variance contained in each the quadrant is also noted.

$$\int P(f)\,df = \int fP(f)\,d[\ln(f)], \tag{1}$$

where $P(f)$ is the spectral power as a function of frequency f. In this plotting convention, integrating across a single row at a given wavenumber gives the spatial mean (area weighted) SLP variance of the spherical harmonic components with the given wavenumber. Integrating down a single column at a given frequency gives the spatial mean (area weighted) variance of the field at the given (discrete) frequency. Because the basis is orthogonal in space and time, integrating across frequency and wavenumber gives the spatial mean (area weighted) variance of the original dataset in the space–time domain.

In the wavenumber–frequency domain, the synoptic variance tends to be a maximum along an axis of increasing wavenumber and higher frequency, which is consistent with the expected nondispersive behavior of disturbances being advected by the mean flow (at the steering level) in the zonal direction. There is very little spectral power at wavenumbers larger than 20 (3% of total variance; not shown in Fig. 1 for visual purposes) and frequencies greater than 0.5 day^{-1} (4% total variance, 1% of which is associated with the diurnal cycle). Therefore, excluding frequencies higher than 0.5 day^{-1} or wavenumbers larger than 20 has very little effect on either the Eulerian or feature tracking statistics.[2]

[2] Feature tracking statistics of daily mean SLP data are nearly identical to the 6-hourly results presented in section 3.

The spatial (temporal) filter divides the wavenumber frequency domain into upper and lower (right and left) portions corresponding to the perturbation and background state fields, respectively, as indicated by the dark black lines in Fig. 1. Together, the spatial and temporal filters divide the variance into four quadrants that are labeled with their associated percent of total variance:

Quadrant I: Small-spatial-scale, high-frequency domain that is common to both filters' definition of the perturbation field.
Quadrant II: Large-spatial-scale, high-frequency domain that is included in the temporal filter's definition of the perturbation field only.
Quadrant III: Large-spatial-scale, low-frequency domain that is excluded from both filters' definition of the perturbation field.
Quadrant IV: Small-spatial-scale, low-frequency domain that is included in the spatial filter's definition of the perturbation field only.

Previous studies have found that the application of the spatial filter only negligibly reduces the variance in the 6-day temporally high-pass filtered field (Hoskins and Hodges 2002), which is equivalent to asking if quadrant II has a significant portion of variance compared to quadrant I. Adjusting the definition of the temporal filter to a 6-day cutoff period in Fig. 1 verifies this result in our dataset (the spatial filter would remove only 8% of the temporal high-pass filtered variance in this case). However, in the definition of the synoptic temporal cutoff used in our study, approximately 40% of the synoptic variance is removed by the spatial filter. Similarly, the temporal filter would eliminate 40% of the variance in the spatially filtered field (the percentage is 75% with the 2–6-day bandpass filter). More generally, Fig. 1 indicates that the variance that is shared by both filtered fields (quadrant I) is smaller than the variance that is included in only one of the filtered fields (quadrants II and IV). Furthermore, there is no clear spectral distinction between the background state and synoptic power in either frequency or wavenumber. Hence, the choice of cutoff wavenumber (frequency) in the spatial (temporal) filter is arbitrary.

Although the temporal filter removes the time-mean field at each grid point, the spatial filter retains the component of the time-mean field that has small spatial scales. The time-mean NDJFM SLP (minus the hemispheric mean) is shown in Fig. 2 (top), along with the part of the field that is retained by the spatial filter (bottom). Hoskins and Hodges (2002) argue that the latter component of the time-mean field should be retained in the field used to identify and track storms because (i) the spatial filter is nearly conservative in the

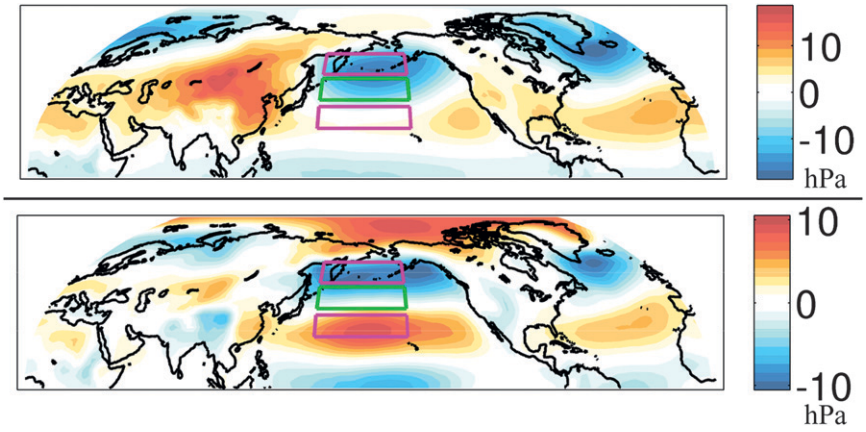

FIG. 2. (top) The time-mean NDJFM SLP field (in hPa) and (bottom) the component of time mean that is greater than planetary wavenumber 5 (hPa). The boxed domains represent the high-, middle-, and low-latitude Pacific domains (used in section 3) over which the time average of the spatially filtered field is negative, neutral, and positive, respectively. The global mean SLP has been removed.

sense that it removes little of the raw data and (ii) they assumed that these time-mean features mainly represent the net effect of passing disturbances rather than stationary planetary waves. These ideas will be pursued in sections 3 and 4, where we will show that (ii) is not true and that retaining this part of time-mean field exerts a profound effect on the feature tracking statistics. For the time being, we note that the retained time-mean field in the spatially filtered data is comparable in magnitude to an average disturbance magnitude (Fig. 8, bottom), and we thus anticipate that its inclusion in the spatially filtered data will play a key role in differentiating the spatially and temporally filtered tracking statistics. Furthermore, in some areas such as the low-latitude North Pacific, the spatially filtered time-mean field departs from and has higher magnitude than the unfiltered time-mean field, reflecting the nonlocal nature of the spatial filter. These are regions where the physical nature of the synoptic storms will be greatly distorted by application of the spatial filter.

3. Tracking results

In the previous section, we showed that the spatial and temporal filters allow different information to be included in the definition of synoptic features and that there are differences in the time-mean fields from which storms/features are defined that are comparable in amplitude to the storms themselves. We now illuminate the differences in the statistics of the storms that arise because of the choice of filter.

Figure 3 shows the magnitude of cyclonic and anticyclonic features defined as the mean filtered magnitude of tracked features passing within a 5° (equatorial) radius of the grid point within the NDJFM season. Figure 3 also shows feature density, which is defined as the number of daily (the tracking data are subsampled at daily intervals to avoid multiple counts at the same location by a single feature) feature locations identified within a 5° radius of a grid point and is given in units of features tracked per month. Feature density counts the same identified feature at multiple time steps, at different locations, and therefore weights slow-moving systems more heavily than rapidly moving systems.

The maximum cyclone magnitude and feature density in the spatially filtered fields occurs in the high-latitude North Pacific. We previously noted that the spatial filter retains a large, negative time mean in this region and we therefore define a region of interest extending from 150°E to 20°W and from 50° to 60°N (poleward purple box in Fig. 2). In contrast, the maximum in anticyclone magnitude and feature density in the spatially filtered fields [neglecting the magnitude maximum in the polar region that was acknowledged to be an artifact of the spatially filtered time mean by Hoskins and Hodges (2002)] occurs in the low-latitude North Pacific, where we previously noted the spatial filter retains a positive time-mean SLP. We therefore define a second region of interest in the low-latitude North Pacific extending from 150°E to 20°W and from 25° to 35°N. We also define a midlatitude region, in between the other two regions, where the time-mean field retained by the spatial filter is relatively neutral (green box in Fig. 2).

In the spatially filtered field, the mean magnitude of the cyclones over the storm track (the high-latitude box) is more than twice the mean magnitude of the

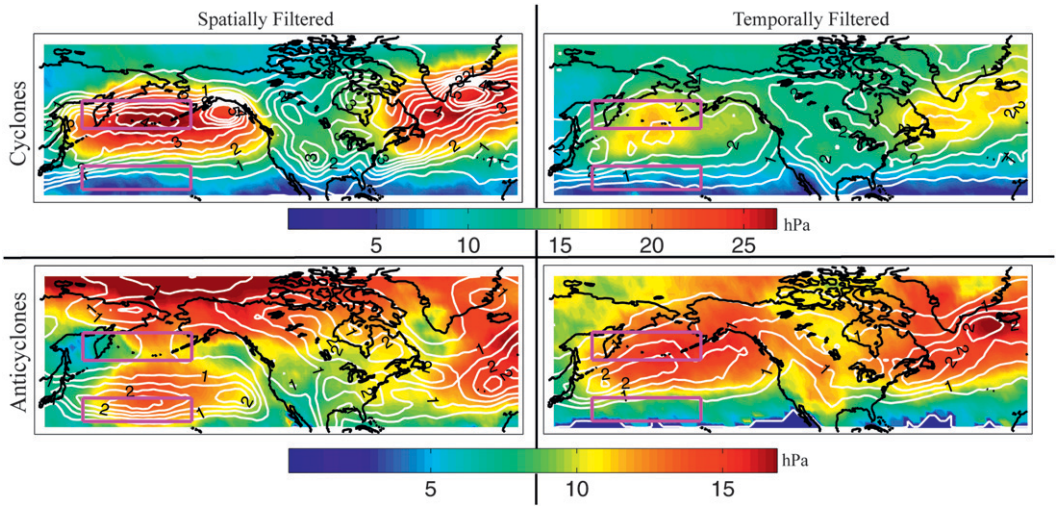

FIG. 3. Magnitude (hPa, color) and feature density (features per month, contoured) for (top) cyclones and (bottom) anticyclones identified by using feature tracking on the (left) spatially and (right) temporally filtered SLP fields. The definition of magnitude and feature density is presented in the text. The purple boxes represent the low- and high-latitude North Pacific domains (also shown in Fig. 2). The contour interval for feature density is 0.5 daily features per month.

anticyclones, whereas the feature density maximum of cyclones and anticyclones is of comparable magnitude. For both cyclones and anticyclones, the maximum in feature density is coincident in space with the maximum in feature amplitude.

The maxima in feature density and mean feature magnitude of anticyclones identified in the spatially filtered fields are shifted about 2000 km south of their cyclonic counterparts. In contrast, using the temporally filtered field, the magnitude and feature density maxima of anticyclones are nearly collocated with those for cyclones. Although the mean magnitude of the cyclones exceeds the mean magnitude of the anticyclones in both the spatially and temporally filtered data, the magnitude asymmetry between cyclones and anticyclones is much more modest in the temporally filtered data (20%) than in the spatially filtered fields (130%). The feature density of the cyclones and anticyclones in the temporally filtered fields have comparable magnitude to each other and to the values in the spatially filtered fields, with the exception of the relatively high cyclone feature density values found in the Gulf of Alaska and southeast of Greenland. The latter regions are coincident with the spatial minima in the time-mean spatially filtered field.

We can get a better picture of how the cyclone/anticyclone magnitude asymmetry relates to the time-mean spatially filtered field by coplotting the two (Fig. 4). Using the spatial prefilter, cyclones have a larger magnitude than anticyclones in the regions where the time average of the spatially filtered SLP is negative; similarly, anticyclones are seen to have (slightly) higher magnitude than cyclones in the (spatially filtered) climatological highs. In the region of maximum storminess (the northern box), the average cyclone magnitude exceeds the average anticyclone magnitude in the spatially filtered field by ~12–14 hPa, which is larger than but comparable to the magnitude of the time-averaged spatially filtered SLP in that region (about 8–10 hPa). Similarly, in the regions of the (spatially filtered) climatological high, the mean anticyclone magnitude exceeds the mean cyclone magnitude in the spatially filtered field by a value that is less than but comparable to the time-mean spatially filtered field in that region. In contrast, the average cyclone/anticyclone magnitude asymmetry in the temporally filtered field has much less spatial structure; it is positive definite, with much smaller magnitude; and it has local maxima in the storm-track entrance regions (typically around 3 hPa), with a minimum in the Gulf of Alaska, where blocking events are known to be common (Rex 1950).

A simple thought experiment in which pure, fixed-magnitude, traveling sine waves of pressure anomalies propagate into a stationary pressure field would lead to a magnitude asymmetry between cyclones and anticyclones of the same magnitude and opposite sign as the stationary pressure field, provided that all features were picked up by the tracking algorithm. The cyclone/anticyclone magnitude asymmetry field in Fig. 4 is systematically higher than this expectation, suggesting there is some synoptic asymmetry between troughs and ridges in the waveform propagating into the time-mean field; the results to this point are consistent with an asymmetric

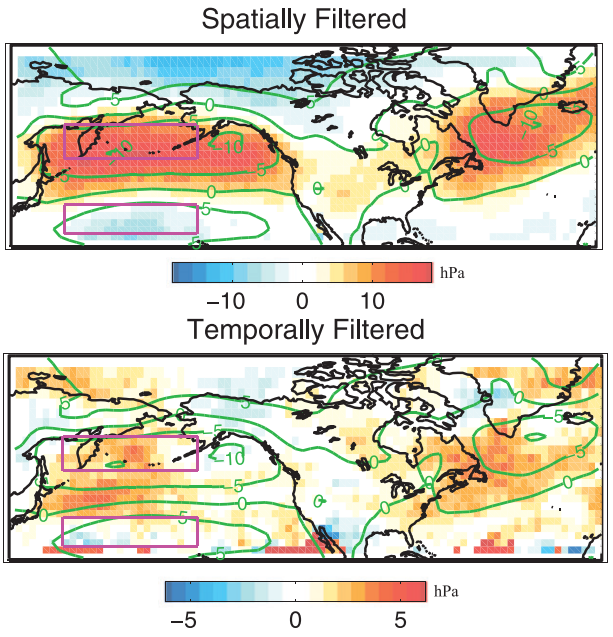

FIG. 4. The difference between the average cyclone magnitude and the average anticyclone magnitude (colors, hPa) for features identified in the (top) spatially and (bottom) temporally filtered SLP. The contours are the time-averaged spatially filtered SLP field (hPa).

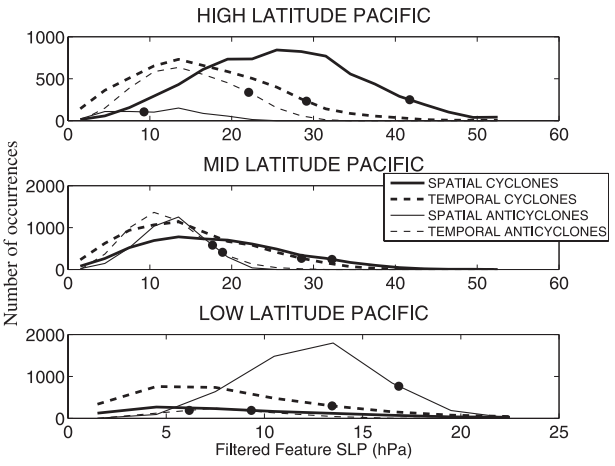

FIG. 5. Feature magnitude histograms for cyclones (thick lines) and anticyclones (thin lines) identified in the spatially (solid lines) and temporally (dashed lines) filtered fields for features identified in the (top) high-, (middle) middle-, and (bottom) low-latitude North Pacific regions, which are defined in the text and boxed in Fig. 2. Each distribution bin spans 3 hPa of feature magnitude. The black dots represent the cutoff storm magnitude for the 400 largest magnitude features in each distribution.

wave form in which troughs are slightly greater in magnitude than ridges (similar to the temporally filtered cyclone/anticyclone asymmetry). It remains to be determined whether the time-mean spatially filtered field represents the net effect of synoptic activity and/or a stationary feature; we will answer this question in section 4.

Histograms of cyclone and anticyclone magnitudes identified in the spatial and temporally filtered fields are shown in Fig. 5 for the high-latitude (top), midlatitude (middle), and low-latitude boxes (bottom). All histogram differences discussed in the subsequent text are significant at the 99% confidence interval, as assessed by the Kolmogorov–Smirnov test (Stuart et al. 1999).

We start by discussing the result in the midlatitude region, where the time-mean spatially filtered SLP is relatively neutral. Here, although the temporal filter identifies more small-magnitude cyclones and anticyclones than the spatial filter, the magnitude histograms of features defined by the two filters are very similar, especially in the large-magnitude tail of the distribution. This suggest that, although the two filters pass different information to the tracking algorithm (Fig. 1), the feature tracking statistics and cyclone/anticyclone magnitude asymmetry defined by the two filters are qualitatively similar in regions where the time-mean spatially filtered field is small.

For the temporally filtered fields within the high-latitude Pacific box (the storm track), the histogram of cyclone magnitude is skewed toward higher magnitudes relative to the histogram of anticyclone magnitudes; both the mean magnitude and number of realizations are higher (about 15% and 35%, respectively) for the cyclones than for the anticyclones. In contrast, in the spatially filtered fields, where the filtered field retains a large negative time-mean SLP in this region (Fig. 2), 10 times as many cyclones as anticyclones are identified and the mean cyclone magnitude is approximately 2½ times the mean anticyclone magnitude. The spatially filtered fields indicate that the high-latitude North Pacific is a region of large cyclone/anticyclone magnitude and frequency asymmetry, whereas the temporally filtered fields indicate that there is only a small asymmetry in this region. The shape of the spatially filtered cyclone magnitude distribution can be well replicated by adding the time-mean spatially filtered SLP field averaged over the high-latitude North Pacific domain (8 hPa) to the temporally filtered cyclone magnitude distribution in the same region. This suggests that cyclone feature tracking in the temporally and spatially filtered fields within the high-latitude North Pacific identifies nearly the same distribution of systems but that the spatially filtered time mean is superimposed on the temporally filtered feature tracking statistics. In contrast, the minute number of anticyclones identified in this region in the spatially filtered field makes the distribution of anticyclones in the spatially and temporally filtered field

irreconcilable; this suggests that the same anticyclones that are identified in the temporally filtered fields are not identified in the spatially filtered fields, most likely because they do not exceed the threshold magnitude because of the strong negative time-mean SLP retained in the spatially filtered data in this region.

In the low-latitude North Pacific, the distribution of cyclones relative to anticyclones in the temporally filtered fields is very similar to the same distributions in the high-latitude Pacific, albeit shifted toward substantially smaller magnitudes than the latter region. The cyclone/anticyclone magnitude asymmetry in the temporally filtered data in this region suggests a modest preference toward enhanced cyclone magnitude and frequency relative to the anticyclones in the same region. In contrast, in the spatially filtered fields within the low-latitude Pacific, where a positive time-mean field is retained, there are nearly 5 times more anticyclones than cyclones identified and the mode of anticyclone magnitude distribution exceeds that of the cyclone magnitude by a factor of 3. The cyclone/anticyclone magnitude and frequency asymmetry in the spatially filtered data over the low-latitude North Pacific is completely opposite the asymmetry seen in the high-latitude Pacific, with a strong preference for anticyclone development. The mode of the spatially filtered anticyclone magnitude distribution is 9 hPa greater than the mode of the temporally filtered anticyclone distribution. The shift toward larger anticyclone magnitudes in the spatially filtered field is consistent with the same systems being tracked in both filtered fields superimposed on the positive time-mean spatially filtered SLP in this region, which has a domain average value of 7 hPa. Furthermore, the number of anticyclones that are identified in the spatially filtered data is drastically larger than the number of anticyclones identified in the temporally filtered data, which also suggests that many of the systems identified in the spatially filtered field do not exceed the minimum threshold (3 hPa) over the requisite tracking period of 3 days in the temporally filtered field.

We have seen that the spatial and temporal filters produce qualitatively different pictures of cyclone/anticyclone asymmetries; this seems to be due to the time-mean field that is retained by the spatial filter. We now ask if composite maps of the tracked features support one interpretation of the feature tracking statistics over the other. We form a composite about the 400 largest magnitude cyclones and anticyclones identified in each the spatially and temporally filtered datasets and within each the low and high-latitude North Pacific domains; the minimum magnitude of the features that are included in constructing the composite in each distribution is indicated by the dots in the histograms (Fig. 5). We chose 400 features to composite over as opposed to a percentage within each distribution because the distributions to be compared have drastically different numbers of realizations; results with 200 or 800 features in each group do not change the conclusions reached. Composite maps are made as follows: (i) take a snapshot of the SLP maps relative to the feature's location at the time the feature is identified; (ii) subtract the winter climatological SLP field from the raw SLP snapshot; and (iii) average over the 400 realizations for the each group. All maps are statistically significant (the composite mean in the vicinity of the extrema exceeds two standard deviations of the individual realizations in that area), although the composite of storms in the temporally filtered data exhibit more variability between the individual realizations than their spatially filtered counterparts.

The composite maps for the high-latitude Pacific are shown in Fig. 6. Visually, both the temporally and spatially filtered cyclones meet our expectations of a synoptic feature; they are meridionally confined and have a zonal wavelength on the order of 50° (~4000 km), which is consistent with the length scale of the most unstable baroclinic modes in the atmosphere (Pedlosky 1998). The spatially filtered anticyclone composite is zonally broader than its temporally filtered counterpart, reflecting the contribution of slow-moving blocking highs to the composite. In both the temporally and spatially filtered fields, we get an impression of cyclones and anticyclones of comparable magnitude, with the cyclones appearing spatially smaller and with a slightly larger magnitude (relative to where the field becomes spatially uniform) than the anticyclones; the composites are consistent with the modest cyclone/anticyclone magnitude asymmetry seen in the features tracked in the temporally filtered data (Fig. 5) and are conclusive evidence that the spatial filter grossly and unphysically distorts the magnitude asymmetry between cyclone and anticyclones.

The composite maps of spatially and temporally filtered cyclones and anticyclones in the low-latitude Pacific (Fig. 7) suggest that both cyclones and anticyclones have smaller magnitudes in this region relative to the high-latitude North Pacific, which is consistent with both the temporally and spatially filtered tracking statistics. The spatially filtered composites have significant spatial structure north of the identified feature location (the origin of the composite); this probably results because spatially filtered anticyclones (cyclones) will tend to all be identified in the center (north) of the domain where the time-mean spatial field has a local maximum (minimum, not shown), and the spatial structure away from the feature reflects the spatial structure of the

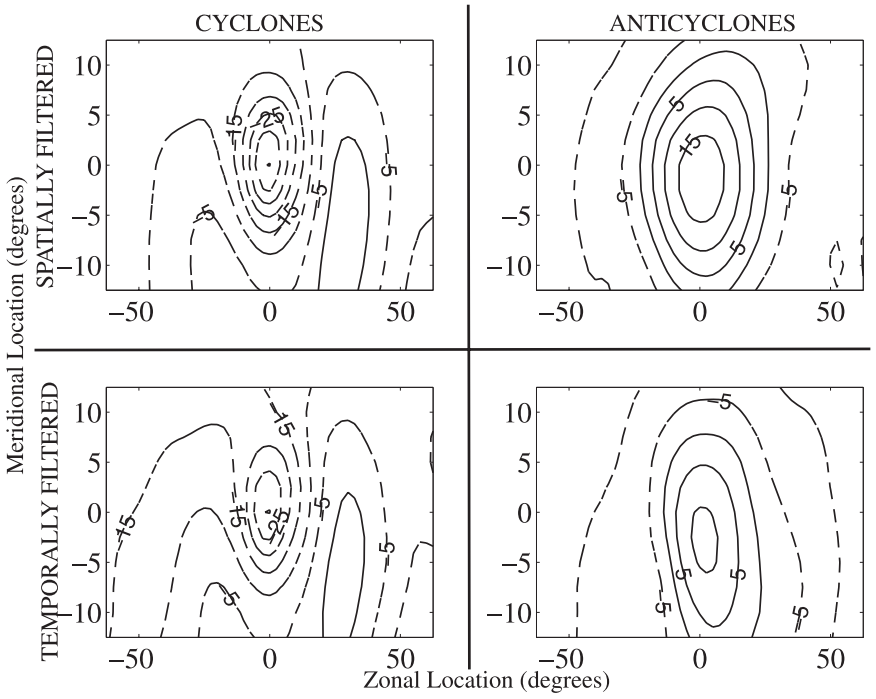

FIG. 6. Composite maps of (left) cyclones and (right) anticyclones in the high-latitude North Pacific box that were identified using feature tracking on the (top) spatially and (bottom) temporally filtered SLP. The contour interval is 5 hPa, with negative values dashed, and climatology has been removed. The zonal and meridional distances are in degrees relative to the features' location.

(subtracted) climatological field. In contrast, the temporally filtered cyclones and anticyclones tend to be evenly dispersed throughout the domain, and the spatial structure of the (subtracted) climatological field is therefore smoothed out. In the low-latitude Pacific, the cyclone and anticyclone composites are zonally narrower than their high-latitude counterparts, which is partially a reflection of the expansion of meridians at equatorward latitudes. In both the spatially and temporally filtered composites, cyclones tend to have a larger central magnitude relative to the background field than anticyclones; this observation is consistent with the cyclone/anticyclone magnitude asymmetry (in favor of cyclones) seen in the temporally filtered feature tracking statistics, and it is strong evidence that the threefold magnitude asymmetry (in favor of anticyclones) seen in the spatially filtered feature tracking statistics is an artifact of (the time-mean field that is retained by) the filter.

4. The contribution of skewness to the time-mean field

In the previous section, we saw that the temporally and spatially filtered SLP fields yielded drastically different feature tracking statistics of cyclone/anticyclone magnitude and frequency asymmetry. We argued that most, but not all, of these differences are attributable to the retention of a portion of the climatological mean field in the spatially filtered field. We now ask if the climatological averaged field (Fig. 2) can be partitioned into a component resulting from stationary features and a component resulting from the net effect of passing synoptic systems and if the latter field coincides with the spatially filtered climatological mean field, as assumed by Hoskins and Hodges (2002) and Anderson et al. (2003).

As a first consideration, we expect that the net contribution of passing disturbances to the time-mean SLP would be proportional to—and bounded in magnitude by—the standard deviation of the Eulerian SLP (Fig. 8, top). This follows from the fact that the net contribution of synoptic waves to the time mean is the mean of the perturbations, which is bounded by the ''typical'' (standard deviation) size of the perturbations, even in a distribution that is very skewed. The map of the standard deviation of SLP indicates that the typical perturbation magnitude is only slightly larger than the time average of the spatially filtered SLP. Hence, it is unlikely that the time-mean field is solely due to the net effect of

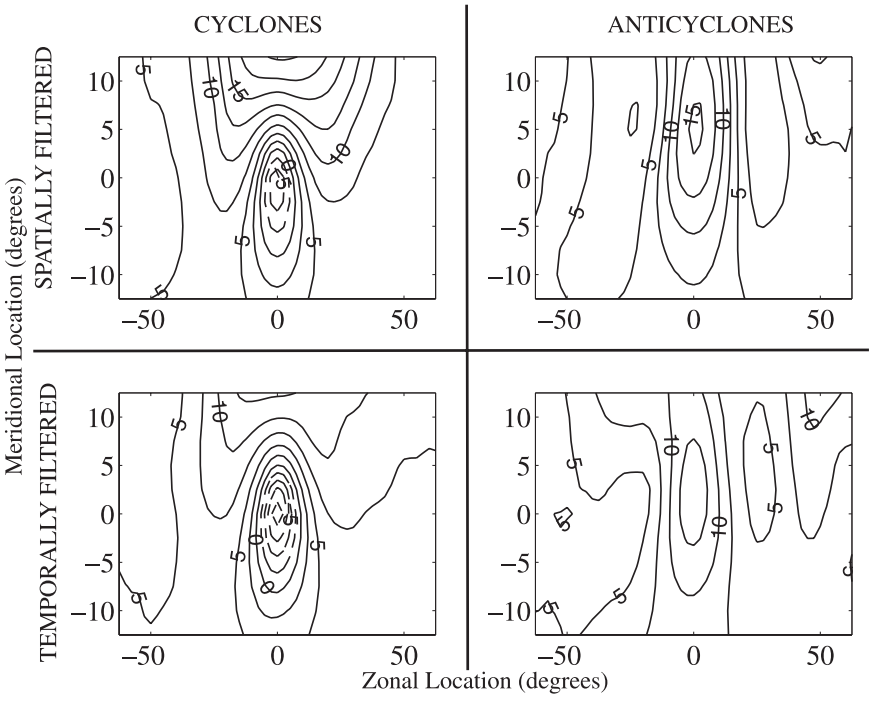

FIG. 7. As in Fig. 6, but for the low-latitude North Pacific and with a contour interval of 2.5 hPa.

passing synoptic waves, even if the average cyclone magnitude was much larger than the average anticyclone magnitude.

The notion that the passing of successive cyclones and anticyclones could lead to a nonzero time mean assumes that there is some asymmetry between the cyclones and anticyclones, because the passing of pure sine waves or other symmetric waveforms results in a zero time mean. Two types of waveform asymmetries exist:

Magnitude asymmetries: If the passing waves tend to have higher magnitude peaks on the positive or negative side, then the time mean will be skewed in that direction.

Persistence asymmetries: If the positive (negative) waveforms are stretched in time relative to the negative (positive) waveforms, then there will be a positive (negative) time mean, even if the magnitudes of the positive and negative waveforms are identical.

In the atmosphere, the implied assumption is that magnitude asymmetries dominate in the storm tracks, because it is commonly believed that synoptic cyclones are deeper than synoptic anticyclones, especially for extreme synoptic events. Although investigations have documented that positive anomalies in the 500-hPa geopotential height are more persistent than negative features (Nakamura and Wallace 1991; Dole and Gordon 1983), there is no published work (to our knowledge) on the role of persistence asymmetries in SLP. We will assume that persistence asymmetries make a negligible contribution to the time-mean SLP and interpret the

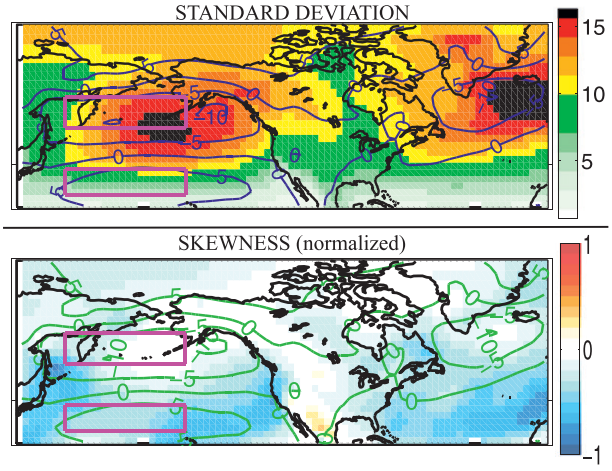

FIG. 8. (top) Standard deviation and (bottom) skewness in the NDJFM SLP. Skewness has been normalized by the cube of the standard deviation and the units of standard deviation are hPa. The contours are the time average of the spatially filtered NDJFM SLP (hPa).

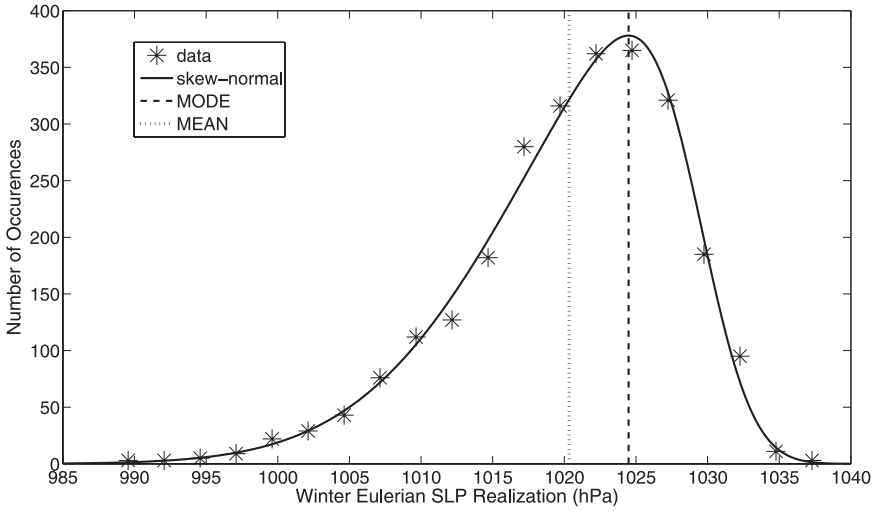

FIG. 9. Histogram of NDJFM SLP data at 35°N, 130°W (asterisks). The solid line is the skew-normal distribution determined by the first three moments of the data: the mean of the distribution (dotted vertical line; 1020.3 hPa), the standard deviation (7.45 hPa), and the normalized skewness (−0.78). The vertical, dashed line is the distribution mode (1024.5 hPa). The offset between the mode and the mean is the contribution to the time mean by the skewness in the disturbances.

results presented later in terms of magnitude asymmetries of synoptic features.

Statistically, it is difficult to isolate the contribution of waveform asymmetries to the time mean, because digital and Fourier filters alike disallow the high-frequency component from having a time mean. Because the cyclone/anticyclone magnitude asymmetry is assumed to manifest itself primarily in extreme synoptic events, we would expect that cyclone/anticyclone magnitude asymmetries would be seen in the tails of an Eulerian pressure distribution, which is indicated by the skewness of the distribution (Fig. 8, bottom); if large-magnitude negative pressure excursions are more frequent than large-magnitude positive pressure excursions, then the skewness will reflect this asymmetry and the time mean will shift toward the negative events. In this framework, the time mean resulting from waveform magnitude asymmetries must be of the same sign as storm skewness, and the time mean resulting from skewness would have a spatial pattern that is very similar to the pattern of normalized (by the variance to the $^3/_2$ power) skewness. We see, however, that the region of minimum time-mean spatially filtered SLP (Fig. 2, bottom) is also a region where skewness is near zero, and the region of maximum time-mean SLP in the spatially filtered data is a region of negative skewness. Hence, it is unlikely that waveform asymmetries contribute to the time-mean SLP.

We now attempt to determine the magnitude and sign of the time-mean field that is due to waveform asymmetries by way of fitting the raw NDJFM SLP distributions at each grid point to a skew-normal distribution.[3] The mean, standard deviation, and skewness of a distribution uniquely define a skew-normal distribution (Azzalini 1985). An example of a skew-normal distribution determined from the first three moments of SLP data at a single grid point is coplotted with a histogram of the data in Fig. 9. If we assume that the skew-normal distribution adequately captures the distribution properties, then the mode of the distribution can be analytically determined from the functional form of the skew-normal distribution.[4]

We next assume that the system is most likely to be in the unperturbed, wave-free state; that is, the mode of the distribution represents the stationary feature. In this framework, we can separate the center of the distribution (in a modal sense) from the part of the time mean that is due to asymmetries in the probability distribution function between positive and negative perturbations (especially in the tails of the distribution); the latter is the difference between the mode and mean and is referred to as contribution to the mean SLP due to skewness. Repeating this procedure at each grid point leads to

[3] We have also performed the subsequent analysis using both spatially and temporally filtered fields, both of which suggest that the contribution of waveform asymmetries to the time-mean field is smaller in magnitude than that calculated using the raw fields.

[4] Fitting the gridpoint histograms to other functional forms of skew distributions (not shown) leads to similar results.

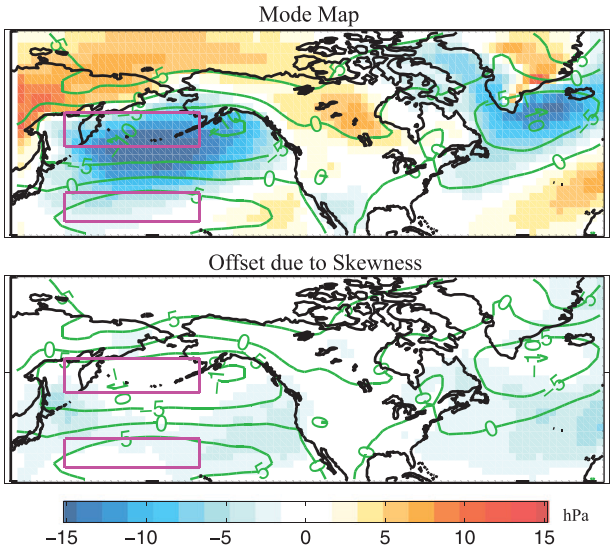

FIG. 10. Map of the mode of NDJFM SLP, which is attributed to (top) stationary waves (color; hPa departure from global mean SLP) and (bottom) offset due to skewness (color; hPa). The contours are the time average of the spatially filtered SLP field (hPa).

maps of the SLP mode and contribution of skewness to the time mean (Fig. 10, top and bottom, respectively).

The mode map resembles the time-mean map in structure and magnitude. The contribution to the mean due to skewness is substantially smaller in magnitude than the observed time mean. Furthermore, in the low-latitude storm-track region, skewness acts to reduce the time-mean high pressure. Hence, the time mean of the spatially filtered fields is not associated with synoptic storms; rather, it is due to stationary waves.[5] These results, combined with those in section 3, clearly show that the application of the spatial filter leads to a gross distortion of the amplitude distribution of cyclones and anticyclones as well as the asymmetry in the amplitude of cyclones and anticyclones.

5. Summary and discussion

Commonly used spatial and temporal filters allow different components of the raw fields to be included in the definition of the synoptic fields. We have shown that, from a variance perspective, the differences in the synoptic variability defined from the spatial and temporal filters are larger than the similarities. Importantly, unlike the temporal filter, the spatial filter admits nonsynoptic features (standing waves) that are collocated with the storm tracks. We show that the nonsynoptic differences in the spatially and temporally filtered data have a large impact on the synoptic dynamics inferred from the analysis of feature tracking using the filtered data.

Using feature tracking on the temporally filtered SLP, we find that there is a modest asymmetry in the magnitude of cyclones and anticyclones, with cyclones being about 20% larger in amplitude than anticyclones in the entire storm-track region. The composite maps of cyclonic and anticyclonic features identified in the temporally filtered SLP qualitatively support this interpretation of the data.

Feature tracking using spatially filtered SLP produces a very different result: cyclones appear to have much greater amplitudes than anticyclones in the regions with climatological low pressure, and anticyclones appear to have much greater amplitudes than cyclones in regions with climatological high pressure. However, compositing the features identified in the spatially filtered fields does not support this interpretation of the data; the composite of the features identified in the spatially filtered data show the same (small) asymmetry in cyclone/anticyclone magnitude as in the temporally filtered data. To identify the cause of the bogus results from feature tracking on the spatially filtered data, we partitioned the time-mean field into a component resulting from stationary features and a component resulting from waveform magnitude asymmetries, and we found that very little of the time-mean field is due to the net effect of passing disturbances. Rather, these experiments suggest that the spatial filter retains a time-mean stationary wave with large-amplitude features coincident with the storm tracks, which is unrelated to the passing of synoptic features and causes the feature tracking eddy statistics to have a grossly distorted view of the dynamics of synoptic disturbances.

These conclusions have implications for feature tracking applications that compare feature tracking statistics from climates with different mean circulations. Because the spatially filtered synoptic fields are biased by

[5] Though we make no attempt at a statistical treatment to assess the validity of assuming the mode of the distribution represents the stationary feature, we now qualitatively discuss the processes that could undermine this assumption. Two observed physical processes are pertinent to misattribution of the distribution mode to the stationary feature: (i) slow-moving or quasi-stationary highs are often observed in the northeastern storm-track regions, whereas quasi-stationary lows are infrequent in the same regions (Nakamura and Wallace 1991) and (ii) synoptic highs tend to be spatially larger than synoptic lows (Hakim and Canavan 2005). In an Eulerian framework, both observations (i) and (ii) would tend to make positive perturbations more likely than negative perturbations, thus shifting the mode toward more positive values relative to stationary feature and leading to a magnitude overestimation of the offset due to skewness in regions of negative skewness. Therefore, we can view our estimate of the offset due to skewness as an upper bound for the time mean because of the net effect of the eddies, given the assumptions we have made.

stationary features, it is likely that comparisons of feature tracking statistics between different climate states will confuse changes in the mean circulation with changes in the eddy statistics. For example, simulations of the Last Glacial Maximum climate system indicate a strengthened Atlantic jet relative to the modern climate (Otto-Bliesner et al. 2006) that is in geostrophic balance with a strong north–south pressure gradient localized to the Atlantic. The spatially filtered time-mean pressure field has a north–south dipole over the Atlantic, similar to the same field in the modern climate (Fig. 2) but with much larger magnitude (not shown). These changes in the mean state that are included in the spatially filtered definition of the synoptic fields overwhelm and bias the true changes in eddy statistics between the different climate states. Comparisons of eddy statistics over the seasonal cycle and for simulations of anthropogenic climate change will suffer from similar confusion between changes in the eddy statistics and background state circulation in the spatially filtered fields. The synoptic fields defined from the temporal filter do not suffer from the same problem.

Although it has been previously noted that the mean magnitudes of cyclones and anticyclones are nearly equal in temporally filtered fields (Anderson et al. 2003), we find that, in the temporally filtered fields, large-magnitude cyclones are more likely to occur than large-magnitude anticyclones. To the extent that the cyclone/anticyclone magnitude asymmetry over the storm-track regions is admitted by the temporally filtered fields, the temporal filter passes skewness perfectly at frequencies relevant to the passing of synoptic features and therefore captures the cyclone/anticyclone magnitude asymmetry with the exception of the component of the time-mean field that is due to the net effect of passing disturbances. We have shown that the latter is a small component (especially in the high-latitude jet exit regions, where synoptic activity is maximized) but that it should nonetheless be accounted for when assessing the true magnitude asymmetry between cyclones and anticyclones. All in all, for tracking of SLP features, this is a minor shortcoming of using the temporal filter compared to the major biases induced by the spatial filter.

We have analyzed the impact of the time mean that is retained when the spatial filter is used on feature tracking statistics of several other variables. In general, we find that the problems identified in the spatially filtered SLP field are equally detrimental in tracking geopotential in the middle troposphere, more problematic in tracking geopotential at upper levels, and less problematic for tracking vorticity features. A simple criteria to assess the impact of the spatial filtering on tracking statistics is to look at the ratio of the retained time-mean field to the standard deviation of the field; if the ratio is greater than or on the order of unity (as is the case for SLP or geopotential at mid- and upper levels), the retained time mean will have a large influence on the tracking statistics.

Our work also has addressed the more fundamental questions: to what extent does the passing of synoptic disturbances contribute to the climatological low pressure centers, and how asymmetric are the probability distribution functions of cyclone and anticyclone magnitude in the storm-track regions? These two questions are nearly inseparable. We have shown that the climatological surface lows are primarily a reflection of stationary features to which the passing of synoptic features make very little contribution, because the raw SLP fields have nearly neutral skewness in these regions. Concurrently, we assert that the weather forecaster's observation that cyclones tend to have larger magnitudes than anticyclones in the storm-track regions is a composite of a true magnitude asymmetry in the propagating waves and the stationary surface pressure features on the poleward flank of the jets. We conclude that the latter is the dominant effect and that the true (dynamical) cyclone/anticyclone magnitude asymmetry in the baroclinic waves is small.

Acknowledgments. We thank Kevin Hodges for the use of his storm-tracking algorithm, Marc Michelsen for his technical support, Greg Hakim for his synoptic insight, and Nicole Feldl for her statistical advice. Sandra Penny provided data and analysis that aided in the conceptual development of this paper. This work was supported by the National Science Foundation's Graduate Student Fellowship program and National Science Foundation Grant ATM-0502204.

REFERENCES

Anderson, D., K. I. Hodges, and B. J. Hoskins, 2003: Sensitivity of feature-based analysis to the form of background field removal. *Mon. Wea. Rev.,* **131,** 565–573.

Azzalini, A., 1985: A class of distributions which includes the normal ones. *Scand. J. Stat.,* **12,** 171–178.

Blackmon, M. L., Y.-H. Lee, and J. M. Wallace, 1984: Horizontal structure of 500 mb height fluctuations with long, intermediate and short-time scales. *J. Atmos. Sci.,* **41,** 961–979.

Blender, R., K. Fraedrich, and F. Lunkeit, 1997: Identification of cyclone track regimes in the North Atlantic. *Quart. J. Roy. Meteor. Soc.,* **123,** 727–741.

Carse, F., and M. Serreze, 1997: Icelandic low cyclone activity: Climatological features, linkages with the NAO, and relationships with recent changes in the Northern Hemisphere circulation. *J. Climate,* **10,** 453–464.

Dole, R. M., and N. D. Gordon, 1983: Persistent anomalies of extratropical Northern Hemisphere wintertime circulation:

Geographical distribution and regional persistence characteristics. *Mon. Wea. Rev.,* **111,** 1567–1586.

Donohoe, A., and D. S. Battisti, 2009: Causes of reduced North Atlantic storm activity in a CCSM3 simulation of the Last Glacial Maximum. *J. Climate,* **22,** 4793–4808.

Hakim, G. J., and A. K. Canavan, 2005: Observed cyclone–anticyclone tropopause vortex asymmetries. *J. Atmos. Sci.,* **62,** 231–240.

——, C. Snyder, and D. J. Muraki, 2002: A new surface model for cyclone–anticyclone asymmetry. *J. Atmos. Sci.,* **59,** 2405–2420.

Hodges, K. I., 1995: Feature tracking on the unit sphere. *Mon. Wea. Rev.,* **123,** 3458–3465.

——, 1999: Adaptive constraints for feature tracking. *Mon. Wea. Rev.,* **127,** 1362–1373.

——, B. J. Hoskins, J. Boyle, and C. Thorncroft, 2003: A comparison of recent reanalysis datasets using objective feature tracking: Storm tracks and tropical easterly waves. *Mon. Wea. Rev.,* **131,** 2012–2037.

Holton, J. R., 2006: *An Introduction to Dynamic Meteorology*. 3rd ed. Academic Press, 535 pp.

Hoskins, B. J., and K. I. Hodges, 2002: New perspectives on the Northern Hemisphere winter storm tracks. *J. Atmos. Sci.,* **59,** 1041–1061.

——, and ——, 2005: A new perspective on Southern Hemisphere storm tracks. *J. Climate,* **18,** 4108–4129.

Kalnay, E., and Coauthors, 1996: The NCEP/NCAR 40-Year Reanalysis Project. *Bull. Amer. Meteor. Soc.,* **77,** 437–471.

Klein, W. H., 1957: Principal tracks and mean frequencies of cyclones and anticyclones in the Northern Hemisphere. U.S. Weather Bureau Research Paper 40, 60 pp.

Köppen, W., 1881: Die Zugstrassen der barometrischen Minima in Europa und auf dem nordatlantischen Ocean und ihr Einfluss auf Wind und auf Wetter bei uns. *Mitt. Geograph. Ges. Hamburg,* **1,** 76–97.

Nakamura, H., and J. M. Wallace, 1991: Skewness of low-frequency fluctuations in the tropospheric circulation during the Northern Hemisphere winter. *J. Atmos. Sci.,* **48,** 1441–1488.

Otto-Bliesner, B. L., E. C. Brady, G. Clauzet, R. Tomas, S. Levis, and Z. Kothavala, 2006: Last Glacial Maximum and Holocene climate in CCSM3. *J. Climate,* **19,** 2526–2544.

Pedlosky, J., 1998: *Geophysical Fluid Dynamics*. 2nd ed. Springer, 710 pp.

Rex, D. F., 1950: Blocking action in the middle troposphere and its effect upon regional climate. I: An aerological study of blocking action. *Tellus,* **2,** 196–211.

Snyder, C., W. C. Skamarock, and R. Rotunno, 1991: A comparison of primitive-equation and semigeostrophic simulation of baroclinic waves. *J. Atmos. Sci.,* **48,** 2179–2194.

Stuart, A., K. Ord, and S. Arnold, 1999: *Classical Inference and the Linear Model*. Vol. 2A, *Kendall's Advanced Theory of Statistics,* Hodder Arnold, 25.37–25.43.

Uppala, S. M., and Coauthors, 2005: The ERA-40 Re-Analysis. *Quart. J. Roy. Meteor. Soc.,* **131,** 2961–3012.

Wallace, J. M., G. H. Lim, and M. L. Blackmon, 1988: Relationship between cyclone tracks, anticyclone tracks, and baroclinic waveguides. *J. Atmos. Sci.,* **45,** 439–462.

Wernli, H., and C. Schwierz, 2006: Surface cyclones in the ERA-40 dataset (1958–2001). Part I: Novel identification method and global climatology. *J. Atmos. Sci.,* **63,** 2486–2507.

——, R. Fehlmann, and D. Lüthi, 1998: The effect of barotropic shear on upper-level induced cyclogenesis: Semigeostrophic and primitive equation numerical simulations. *J. Atmos. Sci.,* **55,** 2080–2094.